# High-Yield Expression and Functional Analysis of *Escherichia coli* Glycerol-3-phosphate Transporter†

Manfred Auer,‡ Myong Jin Kim,‡,§ M. Joanne Lemieux,‡ Anthony Villa,‡,|| Jinmei Song,‡ Xiao-Dan Li,‡,⊥ and Da-Neng Wang*,#

*Skirball Institute of Biomolecular Medicine and Department of Cell Biology, New York University School of Medicine, 540 First Avenue, New York, New York 10016*

*Received January 22, 2001; Revised Manuscript Received March 28, 2001*

ABSTRACT: The glycerol-3-phosphate (G3P) transporter, GlpT, from *Escherichia coli* mediates G3P and inorganic phosphate exchange across the bacterial inner membrane. It possesses 12 transmembrane α-helices and is a member of the Major Facilitator Superfamily. Here we report overexpression, purification, and characterization of GlpT. Extensive optimization applied to the DNA construct and cell culture has led to a protocol yielding ∼1.8 mg of the transporter protein per liter of *E. coli* culture. After purification, this protein binds substrates in detergent solution, as measured by tryptophan fluorescence quenching, and its dissociation constants for G3P, glycerol-2-phosphate, and inorganic phosphate at neutral pH are 3.64, 0.34, and 9.18 $\mu$M, respectively. It also shows transport activity upon reconstitution into proteoliposomes. The phosphate efflux rate of the transporter in the presence of G3P is measured to be 29 $\mu$mol min$^{-1}$ mg$^{-1}$ at pH 7.0 and 37 °C, corresponding to 24 mol of phosphate s$^{-1}$ (mol of protein)$^{-1}$. In addition, the glycerol-3-phosphate transporter is monomeric and stable over a wide pH range and in the presence of a variety of detergents. This preparation of GlpT provides ideal material for biochemical, biophysical, and structural studies of the glycerol-3-phosphate transporter.

The *sn*-glycerol-3-phosphate transporter from *E. coli* mediates G3P[1] to inorganic phosphate exchange across the inner membrane (*1*−*3*). Widely distributed in all phyla (*4*, *5*), GlpT is a member of the Major Facilitator Superfamily (MFS) (*4*, *6*, *7*), the largest secondary transporter family known in the genomes sequenced to date (*4*, *5*). In the cell membrane, these proteins are responsible for the transport of a wide range of solutes, including sugars, amino acids, neurotransmitters, ions, and toxins (*4*, *7*). Medically relevant members of the family include the bacterial efflux pumps associated with antibiotic resistance (*8*, *9*), and the glucose transporter Glut4 in muscle which is linked to diabetes (*10*).

Categorized as a subfamily of the MFS family, the sugar−phosphate/anion antiporters (*11*) mediate the uptake of structurally dissimilar anions, such as hexose phosphates, hexuronates, and glycerol-3-phosphate. Such anion exchange across the membrane constitutes a significant portion of all transport processes in the cell. Yet, with the exception of the human erythrocyte anion exchanger (Band 3) (*12*, *13*), these transporters have not received as much attention as proton- or sodium-driven transport systems. This is due presumably to their low occurrence in natural sources. Of the bacterial anion-exchange systems, the inorganic phosphate ($P_i$)-linked examples, such as the *E. coli* G3P transporter, are among the best characterized (*3*, *14*).

The GlpT protein has 452 amino acids, and its topology is predicted to consist of 12 transmembrane α-helices, with both *N*- and *C*-termini in the cytosol (*15*). These predictions have been validated by *PhoA*- and *LacZ* protein fusion experiments (*16*). The primary sequence of GlpT closely resembles that of the functionally related *E. coli* hexose-6-phosphate transport protein, UhpT, for which a number of functionally important mutations have been identified (*17*−*19*).

GlpT resides in the inner membrane of *E. coli*, and couples the exchange of G3P to $P_i$ (*1*−*3*). G3P is a precursor molecule for phospholipid biosynthesis in bacteria (*20*), and deprivation of this nutrient may result in 90−95% inhibition of phospholipid synthesis in *E. coli* (*21*). It can also serve as the sole carbon and energy source for *E. coli* (*22*). In the absence of G3P, however, the protein retains the ability to mediate $P_i/P_i$ exchange across the membrane. Other substrates identified for the transporter include glycerol-2-phosphate

† This work was supported by NIH Grant RO1-DK53973. M.A. was a recipient of a postdoctoral fellowship from the Human Frontier Science Organization Program and of an Agouron Fellowship in Structural Biology from the Jane Coffin Childs Memorial Fund.

* Correspondence should be addressed to this author at the Skirball Institute of Biomolecular Medicine, New York University School of Medicine, 540 First Ave., New York, NY 10016. E-mail: wang@saturn.med.nyu.edu. Tel.: (212) 263-8634. Fax: (212) 263-8951.

‡ Skirball Institute of Biomolecular Medicine.

§ Present address: ImClone Systems, Inc., 180 Varick St., New York, NY 10014.

|| Present address: Progenics Pharmaceuticals Inc., 777 Old Saw Mill River Rd., Tarrytown, NY 10591.

⊥ Present address: Department of Microbiology, Columbia University, 701 W. 168th St., New York, NY 10032.

# Department of Cell Biology.

[1] Abbreviations: BCA, bicinchoninic acid; BSA, bovine serum albumin; CMC, critical micellar concentration; DDM, dodecylmaltoside; FPLC, fast-performance liquid chromatography; G2P, glycerol-2-phosphate; G3P, glycerol-3-phosphate; GlpT, glycerol-3-phosphate transporter; HPLC, high-performance liquid chromatography; PAGE, polyacrylamide gel electrophoresis; PCR, polymerase chain reaction; $P_i$, inorganic phosphate; PMSF, phenylmethanesulfonyl fluoride; SDS, sodium dodecyl sulfate.

10.1021/bi010138+ CCC: $20.00 
Published on Web 05/10/2001

(G2P), arsenate, and phosphonomycin (*22*). The transport activities of GlpT have been studied in detail by Ambudkar and co-workers (*3*, *11*, *14*, *17*). From liposomes reconstituted with detergent-extracted *E. coli* inner membrane proteins, the G3P-mediated $P_i$ efflux rate has been determined to be 130 nmol $min^{-1}$ (mg of protein)$^{-1}$. The stoichiometry of the substrate exchange by GlpT and its oligomeric state during transport, however, have not been determined (*3*).

The molecular mechanism for substrate transport by GlpT is unclear due to the lack of structural information. In fact, detailed three-dimensional structural information on any member of the entire MFS family is absent. This is due to difficulties encountered in obtaining high expression of such multispan integral membrane proteins, purifying them to homogeneity, and maintaining their stability once removed from the natural lipid environment (*23*). Large amounts of pure detergent-solubilized protein are required for biochemical and biophysical characterization. Indeed, even larger quantities are needed when attempting structural analysis using nuclear magnetic resonance spectroscopy, electron cryo-microscopy, and X-ray crystallography.

Here we report the overexpression, purification, and characterization of the *E. coli* glycerol-3-phosphate transporter. The protocol we established includes: the refinement of DNA constructs, optimization of cell culturing conditions, membrane solubilization, protein purification as well as the introduction of a controlled thrombin protease digestion. The protein is monomeric in detergent solution, and remains active in detergent and following reconstitution into proteoliposomes. The $P_i$ efflux rates mediated by the substrates and their dissociation constants to the transporter have been determined. We have also assessed the stability of the protein over a wide pH range and in a variety of detergents. This preparation may be used for various biophysical and biochemical studies of the transporter protein, including crystallization trials.

## EXPERIMENTAL PROCEDURES

*Overexpression of His-Tagged GlpT: Cloning and Cell Culture.* The GlpT gene was amplified by PCR using *E. coli* DH5α strain as the template, with forward and reverse primers designed according to the published DNA sequence of the protein (*15*). G3P transporter was expressed in the LMG194 strain of *E. coli* using the pBAD expression system containing a *C*-terminal *myc*-epitope and a $His_6$-tag (Invitrogen, Carlsbad, CA) (*24*), following standard molecular biology protocols (*25*).

Limited proteolysis in combination with mass spectroscopy was employed to aid expression construct design (*26*, *27*). Conditions for *E. coli* cell culture were optimized for overexpression with the final GlpT construct, containing amino acids 1−448, followed by a thrombin-specific proteolytic cleavage motif and the *myc*-His-tags. In the optimized protocol, 6 L of LB medium was inoculated with overnight culture and grown for 3 h in the presence of ampicillin, starting at 37 °C. Thirty minutes prior to induction, the culture temperature was gradually lowered to 25 °C, followed by induction at an $OD_{600}$ of 1.0 with 0.1% arabinose. Cells were harvested 90 min after induction, at an $OD_{600}$ of 1.5−1.8.

*Membrane Preparation.* Fresh cell pellet was taken up in TBS buffer (50 mM Tris, pH 8.0, and 400 mM NaCl) containing 0.5 mM phenylmethanesulfonyl fluoride (PMSF) and protease inhibitor cocktail (Sigma, St. Louis, MO), and subjected to 3 cycles of French Press at 18000 psi. The suspension was centrifuged at 15000*g* for 20 min to remove large cellular debris and any remaining unbroken cells, followed by an ultracentrifugation step at 100000*g* for 2.5 h to harvest the membrane. The membrane pellet was stored at −20 °C until future usage.

*Solubilization of Membrane Proteins.* The membrane pellet was solubilized in TBS, 10 mM imidazole, 0.5 mM PMSF, 20% glycerol, and 1% dodecylmaltoside (DDM) (Anatrace, Maumee, OH) for 30 min at 4 °C with stirring, at a ratio of 10 ml of buffer per gram of membrane. The insoluble portion was removed by an ultracentrifugation step at 100000*g* for 30 min.

*$Ni^{2+}$-NTA Affinity Purification and Thrombin Digestion.* Solubilized protein was incubated with $Ni^{2+}$-NTA agarose beads (QIAGEN) for 3 h at 4 °C, with 0.5 ml of resin per gram of membrane. Two washes (20 times the column volume each) were performed with TBS buffer, containing 10 and 15 mM imidazole, respectively. The protein was eluted in 3 steps with 2 times the column volume of the TBS buffer containing 50, 250, and 500 mM imidazole, respectively. The His-tagged protein was detected by Coomassie Blue stained SDS−PAGE and, when necessary, Western-blot analysis using India HisProbe-HRP (Pierce, Rockford, IL). Eluates at 50 and 250 mM imidazole, containing approximately 90% of the total purified GlpT, were combined for subsequent thrombin digestion, which was carried out overnight at 20 °C, using 4 NIH units of thrombin (ICN, Costa Mesa, CA) per milligram of protein.

*Size-Exclusion Chromatography.* After the glycerol concentration was lowered to 5% by dialysis, the thrombin-digested sample was concentrated 16−20-fold to a volume of ∼0.5 ml. The sample was subjected to a preparative size-exclusion Superdex200 column on FPLC (Amersham-Pharmacia, Piscataway, NJ), in the presence of 50 mM imidazole, pH 7.0, 100 mM NaCl, 0.5 mM EDTA, 20% glycerol, and 0.075% DDM. The protein concentration was determined using the Micro-BCA assay (Pierce, Rockford, IL).

*MALDI-TOF Mass Spectrometry.* The molecular mass of purified GlpT protein was measured by matrix-assisted laser desorption/ionization time-of-flight (MALDI-TOF) mass spectrometry (*28*), done in the laboratories of B. Chait in Rockefeller University and of T. Neubert at the Skirball Institute. To avoid interference caused by detergent or lipid, the sample preparation was optimized according to (*29*). Internal calibrants were used to obtain the accurate molecular weight.

*Tryptophan Fluorescence Quenching upon Substrate Binding.* Tryptophan fluorescence quenching of GlpT upon substrate binding was measured from thrombin-digested, SE-column-purified protein, following the published procedure (*30*−*32*). Fluorescence quenching experiments were performed at excitation and emission wavelengths of 283 and 335 nm, respectively, using a FluoroMax-2 fluorometer (Jobin-Yvon-Horiba, Edison, NJ). After establishing the baseline (buffer only) and reference points (protein at 0.01 mg/ml without ligand), the protein solution was titrated with 0.2−320 μM ligand. The effect of dilution (less than 2% of

the total volume) was compensated for at the data processing stage. Changes in fluorescence versus ligand concentration were plotted (*19*, *20*). The binding of the following three substrates was measured: G3P (di-monocyclohexyammonium salt), G2P (sodium salt), or $P_i$, all from Sigma.

*Reconstitution and Transport Assay.* Reconstitution of GlpT into proteoliposomes was carried out according to a modified procedure (*17*, *33*), and the phosphate efflux rate for G3P/$P_i$ or G2P/$P_i$ exchange was measured by monitoring the absorbance changes due to purine phosphorylation by exported inorganic phosphate (*34*). Liposomes were prepared by solubilizing 2 mg of *E. coli* total lipid and egg yolk phosphatidylcholine (ratio 7:1) in the reconstitution buffer (20 mM MOPS, pH 7.0, 5 mM $MgSO_4$, 1 mM DTT, 1% octylglucoside, and 100 mM $KH_2PO_4$), followed by detergent removal upon dialysis. Purified GlpT (1 mg/mL), as well as 0.1% DDM, was added to the liposome suspension until a lipid-to-protein ratio of 200:1 (w/w) was reached. After removal of DDM with 10 mg of Bio-Beads SM2 (Bio-Rad, Hercules, CA), the proteoliposomes were subjected to two freeze−thaw cycles, followed by filtration (0.2 $\mu$m) to eliminate precipitates. The formation and homogeneity of the vesicles were checked by electron microscopy of negatively stained samples (Philips Electron Instruments, Eindhoven, The Netherlands). Subsequently, the reconstituted proteoliposomes were transferred to assay buffer (20 mM MOPS, pH 7.0, 75 mM $K_2SO_4$, 5 mM $MgSO_4$, and 1 mM DTT) using a 10 ml Sephadex G-50 desalting column (Amersham-Pharmacia). Aliquots (100 $\mu$l) of the $P_i$-loaded proteoliposomes were mixed with EnzChek phosphate assay (Molecular Probes, Eugene, OR) to a final volume of 1 ml. The sample was loaded onto a Hewlett-Packard diode array spectrophotometer (model 8453) equipped with a thermostat. After the system reached equilibrium at 37 °C, confirmation of absence of leakage was done by monitoring the absorption at 360 nm; 10 mM each of G3P, G2P, or glycerol was then added, and data were collected at 15 s intervals and adjusted for background. The transport rate was calculated with data collected in the first 60 s after substrate addition, from the linear part of the curve, using the value determined by SDS−PAGE and densitometry for the total amount of the GlpT protein incorporated into proteoliposomes.

*Determination of Oligomeric State and Monodispersity of GlpT.* The oligomeric state and monodispersity of the GlpT protein in various detergent solutions at different pHs were determined by analytical size-exclusion chromatography−HPLC, following a modified protocol in the literature (*32*, *35*−*37*). A 10-fold excess of the buffer was added to the protein solution in order to examine the stability of the protein at various pHs. To study the effects of various detergents on the stability of GlpT, the detergent of interest was added to the protein solution (containing 0.075% DDM) until a final concentration of 0.2% above its critical micellar concentration (CMC) was reached. After 2 h of incubation at 25 °C, the sample was analyzed using a Shodex SW804 size-exclusion chromatography column on HPLC (Waters, Milford, MA) in buffer containing 50 mM Tris, pH 8.0, 200 mM $Na_2SO_4$, 0.05% DDM, and 3 mM $NaN_3$. The Stokes radius of the GlpT−DDM complex was determined using five soluble proteins with known Stokes radii as standards (*36*, *38*, *39*): ferritin (63 Å), amylase (51 Å), aldolase (46 Å), albumin (35 Å), and ovalbumin (28 Å).

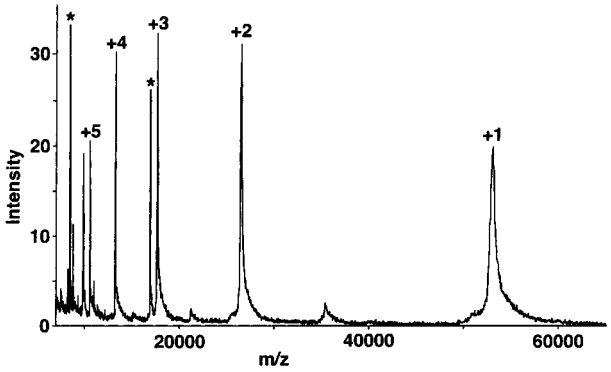


FIGURE 1: Mass spectroscopy of *E. coli* GlpT protein. MALDI-TOF mass spectroscopy was used to help design constructs for expression of GlpT protein in *E. coli*. Initially, the G3P transporter was expressed in a construct containing all 452 amino acids of its wild-type sequence, followed by a *myc*-epitope and a $His_6$-tag. Taking two mutations at the *N*-terminus into account, the expected molecular mass was 53 013 Da. We measured the molecular mass of the expressed protein by MALDI-TOF mass spectroscopy. From the mass of quadruply charged species of 13 254.3 Da, which is between two internal calibrants indicated by a '*', the true molecular mass was found to be 53 017 Da. Indeed, the calculated and experimentally obtained values agree within 4 Da. Limited proteolysis, in combination with mass spectroscopy, was used to identify the rigid core of GlpT protein and to help in designing the expression construct.

## RESULTS

Development of an overexpression system and a purification protocol to produce stable, homogeneous *E. coli* G3P transporter protein required extensive optimization at three different levels. First, a thrombin cleavage site was introduced in the DNA construct, resulting in a protein core that was resistant to further limited proteolysis. Second, a number of parameters were refined at the cell culture stage to eliminate contaminating proteins, which otherwise could not be separated from GlpT by column chromatography. Third, we screened detergent for protein stability and developed a purification protocol consisting of $Ni^{2+}$-NTA affinity chromatography, thrombin digestion, and size-exclusion FPLC. Such a procedure allowed us to produce homogeneous GlpT protein in milligram quantities, which was able to bind substrates in detergent solution and was active after reconstitution into proteoliposomes.

*Cloning and Construct Design.* Mass spectroscopy and trypsin digestion were used to optimize the GlpT expression construct, as has been done for the KscA $K^+$ channel by Doyle et al. (*27*). Initially, the G3P transporter was expressed in the construct GlpT452, where all 452 amino acids of its wild-type sequence were included, followed by a *myc*-epitope and a $His_6$-tag. In the process of cloning and purification, two mutations were detected by *N*-terminal peptide and DNA sequencing: a posttranslationally cleaved *N*-terminal methionine (Met1), as often found with proteins expressed in *E. coli* (*29*); and a Leu2 → Gly2 mutation that was designed for PCR cloning. The actual molecular mass of the expressed protein, therefore, was 53 013 Da. This was confirmed by MALDI-TOF mass spectroscopy measurements, which yielded a value of 53 017 Da (Figure 1). The expected and experimentally measured molecular masses agreed within 4 Da, an error of only 0.07%.

To identify a compact core for later crystallization experiments, $Ni^{2+}$-NTA-purified GlpT452 sample was subjected

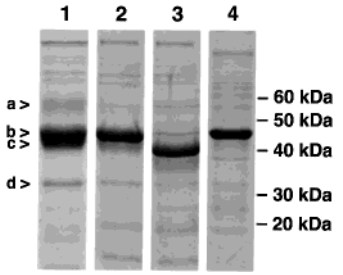


FIGURE 2: Optimization of the *E. coli* cell culture for GlpT overexpression. The GlpT448 (amino acids 1−448) expressed in pBAD vector appeared at a molecular mass of 45 kDa on SDS−PAGE, as indicated by the letter 'b'. Lane 1: When the *E. coli* cells were cultured for 3 h at 37 °C and induced with 0.2% arabinose, an additional 2 h post-induction growth at 37 °C produced a number of contamination bands that could not be separated from GlpT by $Ni^{2+}$-NTA or size-exclusion columns. Two unidentified proteins at 58 and 32 kDa are labeled by the letters 'a' and 'd'. The protein bands indicated by the letter 'c' consisted of proteolyzed GlpT and a broad 'shadow band', appearing 2−3 kDa below the GlpT protein. Lane 2: Reducing the arabinose concentration for induction from 0.2 to 0.1% and lowering the temperature after induction to 25 °C minimized the expression of the 58 and 32 kDa proteins. Shortening the post-induction period from 2 to 1.5 h eliminated the proteolysis problem. Lane 3: The shadow band was a modified version of GlpT which shifted downward by the same distance as GlpT following thrombin digestion. Lane 4: Following a gradual reduction in temperature from 37 to 25 °C half an hour prior to induction, the shadow band disappeared. Samples seen in all lanes were purified by $Ni^{2+}$-NTA affinity chromatography prior to SDS−PAGE.

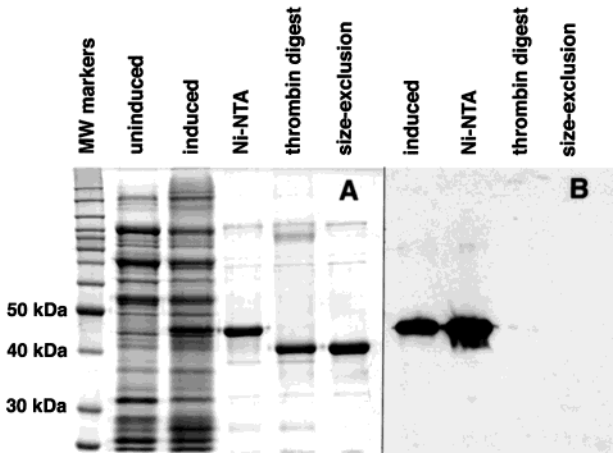


FIGURE 3: Overexpression and purification of the *E. coli* G3P transporter. (A) SDS−PAGE and (B) Western-blot at various stages of expression and purification. Overexpression of GlpT in *E. coli* strain LMG194, with the pBAD vector, was controlled by arabinose. Detergent-solubilized membranes before and after induction with arabinose showed the overexpression of the GlpT protein at a level of 1.8 mg per liter of culture. The expressed GlpT protein was purified using $Ni^{2+}$-NTA affinity chromatography. Following overnight treatment of thrombin at 20 °C, the tags were removed, and the sample was subjected to size-exclusion chromatography. The Western-blot with anti-His probe showed the removal of the tags upon thrombin digestion.

to trypsin treatment at different enzyme-to-protein ratios for various periods of time. Three digestion products ending with residue Arg449, Lys453, and Lys459, respectively, were identified by SDS−PAGE followed by MALDI-TOF mass spectroscopy. Thus, we engineered a DNA construct containing residues 1−448, followed by a thrombin-specific proteolytic site and *myc*-His-tags. Following thrombin digestion of the protein, this GlpT448 construct proved to be resistant to further limited proteolytic treatment by trypsin, chymotrypsin, elastase, and thermolysin. Therefore, we concentrated on this GlpT448 construct in later experiments.

*Expression and Cell Culture.* Growth curves indicated that the middle point of the log phase of cell growth was reached after 3 h at 37 °C. Initially, cells were grown for an additional 2 h following induction with 0.2% arabinose, leading to an $OD_{600}$ of 2.0. The GlpT protein yield obtained was high, at 4−8 mg/l of culture. However, cell culture conditions had to be modified to reduce the amounts of contaminating proteins that could not be separated from GlpT using a two-column chromatography protocol. Further introduction of a third column resulted in protein aggregation, perhaps a result of complete delipidation of GlpT.

Samples purified using $Ni^{2+}$-NTA affinity chromatography were loaded onto SDS−PAGE to assess the quality of GlpT expression and to guide cell culture optimization (Figure 2). GlpT448 ran at 45 kDa, as indicated by the letter 'b'. Two unidentified proteins at 58 kDa, 'a', and 32 kDa, 'd', bound weakly to the $Ni^{2+}$-NTA resin and could not be separated from GlpT by a subsequent size-exclusion or ion-exchange column either. In addition, several sharp bands as well as a broad 'shadow band' appeared 2−3 kDa below GlpT (Figure 2, lane 2, labeled as 'c'). Because the sharp bands resembled those of purified GlpT after controlled trypsin digestion, we concluded that they were GlpT proteolysis products. Upon thrombin digestion, both GlpT and the shadow band shifted by the same distance (Figure 2, lane 3). This suggested that the shadow band was either a posttranslational modification or an *N*-terminal truncation of GlpT.

To eliminate the above-mentioned contaminants, we varied several parameters at the cell culture stage, namely, duration of cell culture, arabinose concentration, and the temperature profile before and after arabinose induction. Reducing the arabinose concentration for induction from 0.2 to 0.1% and lowering the temperature after induction to 25 °C minimized the expression of the 58 and 32 kDa proteins (Figure 2, lane 2). Reducing the post-induction period from 2 to 1.5 h eliminated the proteolysis problem (Figure 2, lane 2). Finally, lowering the temperature from 37 to 25 °C a half hour prior to induction resulted in the complete disappearance of the shadow band (Figure 2, lane 4).

*Solubilization and Purification.* Cell fractionation was carried out by subjecting *E. coli* cells to 3 cycles of French Press, resulting in a breakage of approximately 90% of the cells. Expressed GlpT protein was found in the cell membrane (Figure 3A), as opposed to forming inclusion bodies. A DDM concentration of 1% proved optimal for solubilizing GlpT from the cell membrane.

Optimization of $Ni^{2+}$-NTA affinity purification was achieved by refining the incubation time and defining the optimal protein-to-resin ratio. The protein was bound by incubating the solubilized membrane at 0.5 ml of resin per 1 g of membrane for 3 h. Imidazole at 10 mM was required in the solubilization buffer to reduce unspecific binding. Cumulative optimization of the DNA construct and the cell culture conditions led to ∼90% pure GlpT, free of proteolysis fragments, in the $Ni^{2+}$-NTA affinity chromatography step (Figure 3A). Incubation of the purified GlpT sample with 4 NIH units of thrombin per milligram of protein overnight at 20 °C resulted in complete removal of the *myc*-His-tags, as shown by SDS−PAGE and Western-blot (Figure 3A,B).

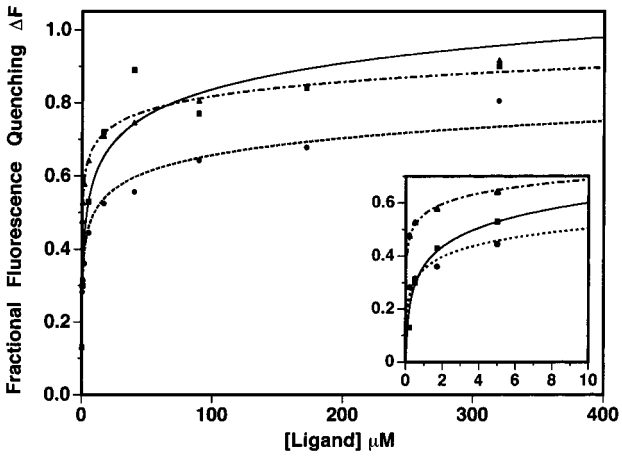


FIGURE 4: Tryptophan fluorescence quenching of GlpT protein upon substrate binding. The substrate was titrated until the fluorescence quenching was saturated, and the fluorescence was measured at excitation and emission wavelengths of 283 and 335 nm, respectively. The binding of three substrates, G3P (squares), G2P (triangles), and $P_i$ (circles), was measured, and their dissociation constants were found to be 3.64, 0.34, and 9.18 $\mu$M, respectively. The details of the data at low substrate concentrations are shown in the inset.

A size-exclusion chromatography step was used to separate the cleaved tags, thrombin protease, and other contaminants. For good separation during size-exclusion FPLC, the protein was applied to the column at ~15 mg/ml concentration. GlpT fractions were collected from the size-exclusion FPLC column at a protein concentration of 2−3 mg/ml. The protein purity was estimated at 95−98%. MALDI-TOF mass spectroscopy showed the preparation to be a sharp, single peak with the expected molecular weight (data not shown), indicating the absence of proteolysis. In summary, 6 l of *E. coli* cell culture typically produced 16 g of cells, resulting in 5 g of membrane after cell fractionation. From this, 10 mg of GlpT could be eluted from a $Ni^{2+}$-NTA affinity column, and 3 mg of pure, stable and monomeric GlpT was recovered from the size-exclusion column.

*Tryptophan Fluorescence Quenching.* To assay the integrity of the GlpT protein in detergent solution, its tryptophan fluorescence quenching upon substrate binding was measured. The affinity of GlpT in solution was determined for the substrates G3P, G2P, and $P_i$ (Figure 4), and their dissociation constants at neutral pH were found to be 3.64, 0.34, and 9.18 $\mu$M, respectively. Scatchard plot analysis of these data indicated one binding site per GlpT molecule for all three substrates (data not shown).

*Reconstitution into Vesicles and Transport Assay.* Reconstitution of GlpT into vesicles was achieved by mixing preformed lipid vesicles and solubilized GlpT in the presence of detergent. This was followed by the removal of the detergent using Bio-Beads. The GlpT proteoliposomes containing phosphate buffer were round, uniform, and unilamellar with a diameter of 200−400 nm, as visualized by electron microscopy (Figure 5, inset). We measured the transport of phosphate across the lipid membrane of reconstituted proteoliposomes, using a commercially available enzymatic assay (*34*). Circumventing the use of any radioactive substrate, the efflux of inorganic phosphate leads to enzymatically catalyzed phosphorylation of a reporter substrate, which subsequently absorbs light at a wavelength of

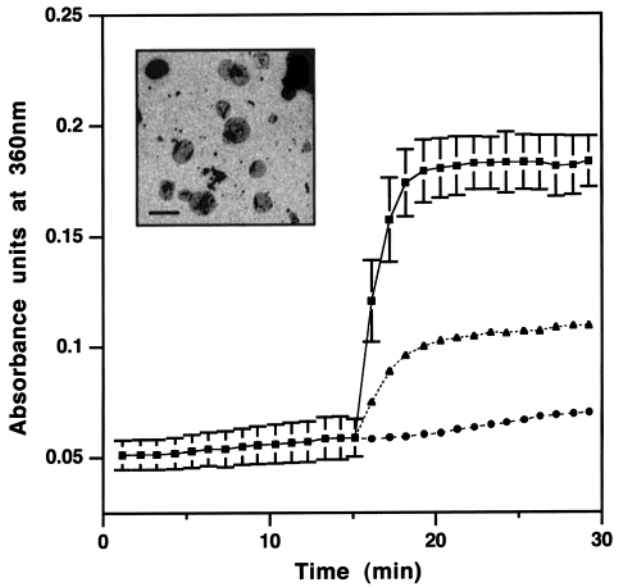


FIGURE 5: Phosphate transport mediated by GlpT protein. Inorganic phosphate efflux in absorbance units was measured in $P_i$-loaded and GlpT-reconstituted proteoliposomes upon the addition of substrate to the assay solution. An electron micrograph of the proteoliposomes is shown in the inset (scale bar in the inset = 100 nm). $P_i$ efflux against substrate was measured via the absorbance at 360 nm at 37 °C, at 15 s intervals. The system was monitored for 15 min to detect leakage, directly followed by an additional 15 min after the addition of G3P (squares), G2P (triangles), or glycerol (circles). Error bars represent the standard error from measurements performed in triplicate (G3P) or duplicate (G2P). The $P_i$ efflux rate was found to be 29 $\mu$mol $min^{-1}$ $mg^{-1}$ for G3P, and 8.9 $\mu$mol $min^{-1}$ $mg^{-1}$ for G2P. Glycerol did not initiate phosphate transport.

360 nm. As indicated in Figure 5, $P_i$ did not leak from the proteoliposomes. Only after the addition of G3P or G2P was inorganic phosphate detected outside of the liposomes. The G3P-mediated $P_i$ efflux rate was found to be 29 $\mu$mol $min^{-1}$ (mg of protein)$^{-1}$ at 37 °C, equivalent to a turnover rate of 24 mol of $P_i$ $s^{-1}$ (mol of GlpT)$^{-1}$. The $P_i$ efflux rate for G2P/$P_i$ exchange was 8.7 $\mu$mol $min^{-1}$ $mg^{-1}$, corresponding to 7.4 mol of $P_i$ $s^{-1}$ (mol of GlpT)$^{-1}$. Glycerol, as a control, did not initiate phosphate transport.

*Characterization of Oligomeric State and Stability of Purified GlpT.* The oligomeric state and stability of detergent-solubilized GlpT were characterized by analytical size-exclusion HLPC (*32*, *35*−*37*). Judged from its retention time on the size-exclusion column, GlpT was monomeric in DDM detergent solution (Figure 6A). The Stokes radius of the GlpT−DDM complex was 46 ± 5 Å, using soluble proteins as standards. Comparing with two other membrane transporter proteins with both a similar molecular mass and number of transmembrane α-helices, 75 Å for dimeric Band 3 membrane domain in DDM (2 × 53 kDa and 2 × 14 helices) (*35*) and 50 Å for monomeric erythrocyte glucose transporter in DM (54 kDa and 12 helices) (*32*), we concluded that the GlpT protein in DDM solution was a monomer.

The effects of pH and detergent on the stability and oligomeric state of the protein were also monitored by size-exclusion HPLC. As seen in Figure 6B, GlpT was monomeric across a range of pH from 4.5 to 8.5; in contrast, at pH 3.5 and 9.5, aggregation occurred. We also tested 15 different detergents at neutral pH and have found that GlpT was either monomeric or aggregated, depending on the

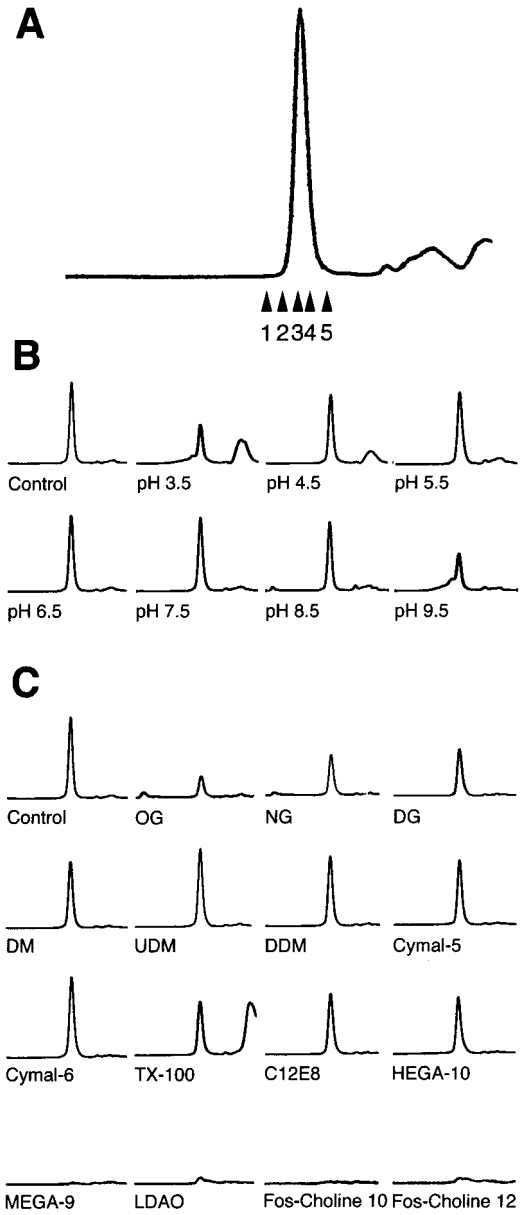


FIGURE 6: Oligomeric state and monodispersity of GlpT protein under different conditions. (A) GlpT is a monomer in solution. Analytical size-exclusion chromatography demonstrated that GlpT protein purified in DDM detergent as monomer. The GlpT−DDM complex was found to have a Stokes radius of 46 ± 5 Å. Five soluble proteins of known Stokes radius were used for calibration: (1) ferritin (63 Å); (2) amylase (51 Å); (3) aldolase (46 Å); (4) albumin (35 Å); (5) ovalbumin (28 Å). (B) Stability of GlpT protein at different pHs. The protein stayed monodisperse over a wide pH range: pH 4.5−8.5. (C) Stability of GlpT protein in different detergents. The protein remained as a monomer in a number of detergents: decylglucoside (DG), decylmaltoside (DM), undecylmaltoside (UDM), dodecylmaltoside (DDM), Cymal-5, Cymal-6, Triton-100, $C_{12}E_8$, and HEGA-10. The controls were kept at 4 °C. All other samples were prepared by incubation at the desired pH for (B), or in the presence of the detergent for (C), for 2 h before HPLC measurement.

detergent added (Figure 6C). The purpose of this study was to identify detergents capable of maintaining the protein in a monodisperse state for later crystallization experiments. The following results were observed: All five maltoside-based detergents of different aliphatic chain length were capable of keeping GlpT monodisperse. More specifically, GlpT in undecylmaltoside showed the narrowest peak, closely followed by dodecylmaltoside, Cymal-6, Cymal-5, and decylmaltoside. Comparable results have been obtained with the three glucoside-based detergents tested, i.e., decylglucoside, nonylglucoside, and octylglucoside. Other detergents able to keep the protein monodisperse were Triton-X100, $C_{12}E_8$, and HEGA 10, whereas MEGA 9, LDAO, FOS-Choline 10, and FOS-Choline 12 led to aggregation. In addition, GlpT in DDM stayed monodisperse for over 4 weeks at 4 °C, and more than 10 days at 25 °C. The protein was able to tolerate several cycles of freezing and thawing.

## DISCUSSION

We have successfully overexpressed the *E. coli* sugar−phosphate transporter GlpT, a member of the Major Facilitator Superfamily (*4*). By changing various parameters during cell culture, we have minimized the expression of proteolytic products, posttranslationally modified GlpT, and other contaminants. The protein after purification appears active upon reconstitution into liposomes, as shown by a nonradioactive transport assay, and is also capable of binding substrates in its detergent-solubilized state, as demonstrated by fluorescence quenching. Therefore, the protein does not undergo substantial structural changes during solubilization and purification, providing ideal material for biophysical and biochemical characterization, including 3D crystallization.

Measured by fluorescence quenching, the dissociation constants of GlpT for G3P, G2P, and $P_i$ at neutral pH, are 3.64, 0.34, and 9.18 $\mu$M, respectively (Figure 4), indicating its affinity is highest for G2P and lowest for $P_i$ among the three substrates tested. These results complement rather well with those obtained by the transporter assay of reconstituted proteoliposomes (Figure 5). The G3P-mediated $P_i$ efflux rate of the GlpT protein measured from proteoliposomes, 29 $\mu$mol $min^{-1}$ (mg of protein)$^{-1}$, or 24 mol of $P_i$ $s^{-1}$ (mol of GlpT)$^{-1}$, is consistent with the rate of other secondary transporters (*40, 41*). The $P_i$ efflux rate in the presence of G2P, 8.7 $\mu$mol $min^{-1}$ $mg^{-1}$, is significantly lower than the rate for G3P/$P_i$ antiport. This is expected since the GlpT protein shows a higher affinity for G2P than for G3P (Figure 4). Furthermore, the saturation of transport observed for G2P and G3P in Figure 5 was due, presumably, to equilibrium of the substrates inside and outside the proteoliposomes. A substrate with a higher affinity will bind to the protein at a lower internal concentration in the proteoliposomes, resulting in competitive binding (*11*). Therefore, compared to G3P, G2P saturates GlpT earlier in the efflux assay, resulting in a lower external $P_i$ concentration at saturation (Figure 4). The G3P-mediated $P_i$ efflux rate reported here, however, is 2 orders of magnitude greater than that reported by Ambudker et al. (*3*). Their value is estimated indirectly from $K_m$ determined from reconstituted whole cell membrane, while ours is measured directly from proteoliposomes reconstituted from purified G3P transporter.

Another interesting point is the stoichiometry for substrate exchange. In addition to mediating G3P/$P_i$ antiport across the cell membrane, GlpT has been shown to exchange $P_i$ for $P_i$ (*3*). Since this transporter is not electrogenic, the stoichiometry for the substrate exchange of GlpT is therefore likely to be 1:1, although it has not been unambiguously determined. There is evidence that the stoichiometry for the system responsible for hexose-6-phosphate/$P_i$ exchange in

*Streptococcus lacti* varies between 1:1 and 1:2 in a pH-dependent manner. The reconstitution protocol using purified GlpT, as reported here, provides an excellent system to clarify this question in the future.

The monomeric GlpT in detergent solution is likely to represent the basic functional unit of the protein in the cell membrane, as in the case of the Lac permease (*41*) and human erythrocyte glucose transporter (*42*), two of the best-characterized members of the Major Facilitator Superfamily. However, our result is in discordance with a previous report, where, based on genetic evidence, the protein was suggested to be oligomeric (*2*). Differences in the oligomeric state of the protein in lipid bilayer versus detergent solution cannot be ruled out. However, the fact that the solubilized protein is still able to bind substrates and resume transport activity upon reconstitution into liposomes suggests that the protein may function as a monomer.

We have characterized the protein's monodispersity within a broad pH range and in a variety of detergent solutions. The protein is monomeric between pH 4.5 and 8.5, and does not oligomerize or aggregate in the presence of various detergents, as demonstrated by its behavior in size-exclusion HPLC analysis. It should be noted, however, that a small fraction of dimeric GlpT has been observed at pH 3.5 and 9.5 but since these pH values are nonphysiological we doubt the significance of this finding. In monodispersity studies in various detergents, the concentration of the detergent of interest is 0.2−1.0% and therefore much higher than the concentration of DDM (0.075%) present. The behavior of the protein observed, therefore, reflects primarily the effects of the detergent being examined, instead of the original DDM detergent present. Since the monodispersity of a protein preparation is believed to increase it crystallizability (*43*), the large number of detergents that keep GlpT stable provides ample possibilities for crystallization trials.

Glycerol-3-phosphate is a major precursor for lipid synthesis in eukaryotic cells (*44*), and is involved in physiological processes such as the regulation of metabolism of the low-density lipoprotein (LDL) (*45*). Comparison of GlpT with the human glycerol-3-phophate transporter (*SLC37*) (*46*) reveals an overall low homology, with regions of higher sequence conservation (up to 36% identity) in the loops connecting transmembrane regions 4 and 6 as well as 6 and 7. Although the human and bacterial G3P transporters share limited sequence homology and are evolutionary distant, they both transport the same substrate and most likely share a similar structure and transport mechanism. A similar situation has been found for two members of the seven-transmembrane proteins, bacteriorhodopsin and rhodopsin, whose 3D structures have been determined to atomic resolution (*47*, *48*). Although their amino acid sequences seem unrelated, they adopt a remarkably similar structure. Consequently, bacteriorhodopsin and, more recently, rhodopsin have been used as starting models for many homology-modeling efforts of the pharmacologically important G-protein-coupled membrane proteins. The main aim of our efforts is the structure determination of GlpT at high resolution and subsequent homology-modeling of other medically important members of the MFS family.

The protocol we report here is novel to the extent that the optimization of cell culture conditions is used as a way to eliminate microheterogeneity due to posttranslational modification, as often occurs when overexpressing membrane transporter proteins (*49*, *50*). We hope that the protocol, which has allowed us to obtain pure, homogeneous, stable G3P transporter protein, will stimulate and enable other investigators to overcome the problems one usually encounters when working with this particularly difficult class of proteins.

## ACKNOWLEDGMENT

We thank Martine Cadene, Yun Lu, and Thomas Neubert for MALDI-TOF mass spectroscopy measurements, Mathieu Schapira for help in sequence alignment, and Heather Griffith for critical reading of the manuscript.

## REFERENCES

1. Silhavy, T. J., Hartig-Beecken, I., and Boos, W. (1976) *J. Bacteriol. 126*, 951−958.
2. Larson, T. J., Schumacher, G., and Boos, W. (1982) *J. Bacteriol. 152*, 1008−1021.
3. Ambudkar, S. V., Larson, T. J., and Maloney, P. C. (1986) *J. Biol. Chem. 261*, 9083−9086.
4. Saier, M. H., Jr., Beatty, J. T., Goffeau, A., Harley, K. T., Heijne, W. H., Huang, S. C., Jack, D. L., Jahn, P. S., Lew, K., Liu, J., Pao, S. S., Paulsen, I. T., Tseng, T. T., and Virk, P. S. (1999) *J. Mol. Microbiol. Biotechnol. 1*, 257−279.
5. Paulsen, I. T., Nguyen, L., Sliwinski, M. K., Rabus, R., and Saier, M. H., Jr. (2000) *J. Mol. Biol. 301*, 75−100.
6. Henderson, P. J. F. (1993) *Curr. Opin. Cell Biol. 5*, 708−712.
7. Marger, M. D., and Saier, M. H., Jr. (1993) *Trends Biochem. Sci. 18*, 13−20.
8. Cheng, J., Hicks, D. B., and Krulwich, T. A. (1996) *Proc. Natl. Acad. Sci. U.S.A. 93*, 14446−14451.
9. Walsh, C. (2000) *Nature 406*, 775−781.
10. Kahn, B. B. (1992) *J. Clin. Invest. 89*, 1367−1374.
11. Maloney, P. C., Ambudkar, S. V., Anatharam, V., Sonna, L. A., and Varadhachary, A. (1990) *Microbiol. Rev. 54*, 1−17.
12. Reithmeier, R. A., Landolt-Marticorena, C., Casey, J. R., Sarabia, V. E., and Wang, J. (1993) *Soc. Gen. Physiol. Ser. 48*, 161−168.
13. Wang, D. N. (1994) *FEBS Lett. 346*, 26−31.
14. Ambudkar, S. V., Sonna, L. A., and Maloney, P. C. (1986) *Proc. Natl. Acad. Sci. U.S.A. 83*, 280−284.
15. Eiglmeier, K., Boos, W., and Cole, S. T. (1987) *Mol. Microbiol. 1*, 251−258.
16. Gott, P., and Boos, W. (1988) *Mol. Microbiol. 2*, 655−663.
17. Ambudkar, S. V., and Maloney, P. C. (1986) *Methods Enzymol. 125*, 558−563.
18. Fann, M. C., and Maloney, P. C. (1998) *J. Biol. Chem. 273*, 33735−33740.
19. Hall, J. A., Fann, M. C., and Maloney, P. C. (1999) *J. Biol. Chem. 274*, 6148−6153.
20. Rock, C. O., and Cronan, J. E. (1985) in *Biochemistry of Lipids and Membranes* (Vance, D. E., and Vance, J. E., Eds.) pp 73−115, Benjamin/Cummings, Menlo Park, CA.
21. Ray, T. K., and Cronan, J. E. J. (1987) *J. Bacteriol. 196*, 2896−2898.
22. Elvin, C. M., Hardy, C. M., and Rosenberg, H. (1985) *J. Bacteriol. 161*, 1054−1058.
23. Grisshammer, R., and Tate, C. G. (1995) *Q. Rev. Biophys. 28*, 315−422.
24. Guzman, L. M., Belin, D., Carson, M. J., and Beckwith, J. (1995) *J. Bacteriol. 177*, 4121−4130.
25. Sambrook, J., Fritsch, E. F., and Maniatis, T. (1989) *Molecular Cloning. A Laboratory Manual*, 2nd ed., Vol. 1, CSHL Press, New York.
26. Wei, L., Hubbard, S. R., Hendrickson, W. A., and Ellis, L. (1995) *J. Biol. Chem. 270*, 8122−8130.
27. Doyle, D. A., Morais Cabral, J., Pfuetzner, R. A., Kuo, A., Gulbis, J. M., Cohen, S. L., Chait, B. T., and MacKinnon, R. (1998) *Science 280*, 69−77.

28. Cohen, S. L., and Chait, B. T. (1997) *Anal. Biochem. 247*, 257−267.
29. Cadene, M., and Chait, B. (2000) *Anal. Chem. 72*, 5655−5658.
30. Chin, J. J., Jhun, B. H., and Jung, C. Y. (1992) *Biochemistry 31*, 1945−1951.
31. Walmsley, A. R., Lowe, A., and Henderson, P. J. F. (1994) *J. Biochem. 221*, 513−522.
32. Boulter, J. M., and Wang, D. N. (2001) *Protein Expression Purif.* (in press).
33. Rigaud, J.-L., Pitard, B., and Levy, D. (1995) *Biochim. Biophys. Acta 1231*, 223−246.
34. Webb, M. R. (1992) *Proc. Natl. Acad. Sci. U.S.A. 89*, 4884−4887.
35. Casey, J. R., and Reithmeier, R. A. (1993) *Biochemistry 32*, 1172−1179.
36. Harlan, J. E., Picot, D., Loll, P. J., and Garavito, R. M. (1995) *Anal. Biochem. 224*, 557−563.
37. Taylor, A. M., Boulter, J., Harding, S. E., Colfen, H., and Watts, A. (1999) *Biophys. J. 76*, 2043−2055.
38. Kranz, D., Mutzbauer, H., and Schulz, G. V. (1965) *Biochim. Biophys. Acta 102*, 514−525.
39. Le Maire, M., Aggerbeck, L. P., Monteilhet, C., Andersen, J. P., and Moller, J. V. (1986) *Anal. Biochem. 154*, 525−535.
40. Scarborough, G. A. (1985) *Microbiol. Rev. 49*, 214−231.
41. Kaback, H. R., and Wu, J. (1997) *Q. Rev. Biophys. 30*, 333−364.
42. Burant, C. F., and Bell, G. I. (1992) *Biochemistry 31*, 10414−10420.
43. Ferre-D'Amare, A. R., and Burley, S. K. (1994) *Structure 2*, 357−359.
44. Vance, D. E. (1985) in *Biochemistry of Lipids and Membranes* (Vance, D. E., and Vance, J. E., Eds.) pp 242−70, Benjamin/Cummings, Menlo Park, CA.
45. Heimberg, M., Olubadewo, J. O., and Wilcox, H. G. (1985) *Endocr. Rev. 6*, 590−607.
46. Bartoloni, L., Wattenhofer, M., Kudoh, J., Berry, A., Shibuya, K., Kawasaki, K., Wang, J., Asakawa, S., Talior, I., Bonne-Tamir, B., Rossier, C., Michaud, J., McCabe, E. R., Minoshima, S., Shimizu, N., Scott, H. S., and Antonarakis, S. E. (2000) *Genomics 70*, 190−200.
47. Henderson, R., Baldwin, J. M., Ceska, T. A., Zemlin, F., Beckmann, E., and Downing, K. H. (1990) *J. Mol. Biol. 213*, 899−929.
48. Palczewski, K., Kumasaka, T., Hori, T., Behnke, C. A., Motoshima, H., Fox, B. A., Le Trong, I., Teller, D. C., Okada, T., Stenkamp, R. E., Yamamoto, M., and Miyano, M. (2000) *Science 289*, 739−745.
49. Racher, K. I., Voegele, R. T., Marshall, E. V., Culham, D. E., Wood, J. M., Jung, H., Bacon, M., Cairns, M. T., Ferguson, S. M., Liang, W. J., Henderson, P. J., White, G., and Hallett, F. R. (1999) *Biochemistry 38*, 1676−1684.
50. Tamai, E., Fann, M. C., Tsuchiya, T., and Maloney, P. C. (1997) *Prot. Expr. Purif. 10*, 275−181.

BI010138+